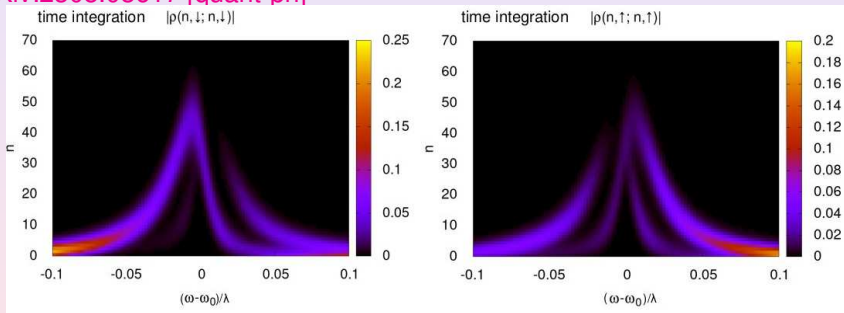


Quantum synchronization and entanglement of dissipative qubits coupled to a resonator



Alexei Chepelianskii (LPS CNRS) & Dima Shepelyansky (LPT Toulouse)
www.quantware.ups-tlse.fr/dima

arXiv:2308.03617 [quant-ph]



resonator photon population vs detuning, Lindblad computations, up to 4 millions components

Other OCTAVES pubs: K.Frahm, DS: Eur. Phys. J. D **75**, 277(2021) [chaotic EPR pairs]; J. Phys. A: Math. Theor. **55**, 234004 (2022) [Loschmidt echo]

Support: ANR OCTAVES + LABEX NANOX MTDINA project (disruptive)

Synchronization Huygens 1665

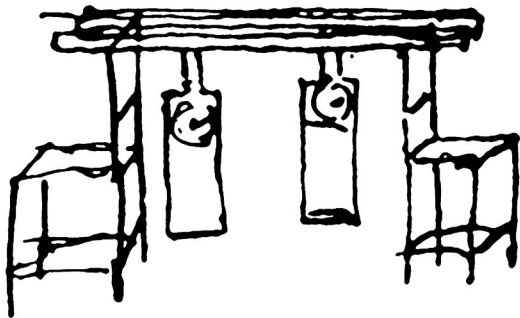


Figure ... Original drawing of Christiaan Huygens illustrating his experiments with two pendulum clocks placed on a common support.

First recognized in 1665 by Christiaan Huygens, synchronization phenomena are abundant in science, nature, engineering, and social life.

Pikovsky et al. *Synchronization*, Cambridge Univ. Press (2001)

The Royal Society's founding in 1660, Christiaan Huygens, set out to solve the outstanding technological challenge of the day: the longitude problem, i.e. finding a robust, accurate method of determining longitude for maritime navigation. → clock accuracy

various systems ranging from clocks to fireflies, cardiac pacemakers, lasers and Josephson junction (JJ) arrays ...

Quantum synchronization (QSYNC) - first steps

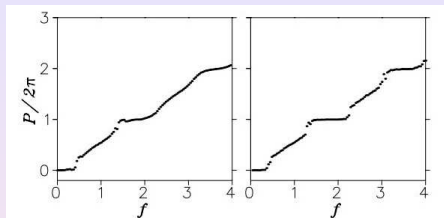


Fig. 5. Dependence of the average momentum P on static force f at $K = 0.8$, $\gamma = 0.25$ (compare with the data in Fig. 1, left column). Right: quantum case at $\hbar = 0.05$ (same data as in Fig. 1, left column). Left: classical simulation of classical

PRL **100**, 014101 (2008)

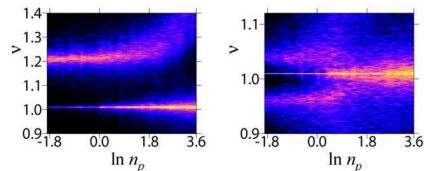


FIG. 6 (color online). Spectral density $S(\nu)$ of qubit radiation $\xi_z(t)$ as function of driving power n_p in the presence of phase noise in ϕ with diffusion rate $\eta = 0.004\omega_0$. Left: $\Omega/\omega_0 = 1.2$; right: $\Omega/\omega_0 = 1$. Other parameters are as in Fig. 1. Grayness

Zhiron, DS Eur. Phys. J. D **38**, 375 (2006)

[dissipative quantized map, analog of Shapiro steps - fig left];

PRL **100**, 014101 (2008) [qsync for qubit+driven resonator - fig right];

PRB **80**, 014519 (2009) [2 qubits + driven resonator \rightarrow entangled qubits]

Approach and weak points:

method of quantum trajectories, qubits were non-dissipative

QSYNC Lindblad model: driven resonator + qubits

Hamiltonian: λ coupling, $\omega, \omega_0, \Omega_l$ driving, resonator, qubits freq-s
(extended Jaynes-Cummings model)

$$\hat{H}(t) = \hbar\omega_0\hat{a}^+\hat{a} + \hbar\sum_l\lambda_l\hat{\sigma}_{x,l}(\hat{a} + \hat{a}^+) + \sum_l\frac{\hbar\Omega_l}{2}\hat{\sigma}_{z,l} + 2F(\hat{a} + \hat{a}^+)\cos\omega t$$

RWA stationary Hamiltonian:

$$\hat{H}_{\mathcal{R}} = \hbar(\omega_0 - \omega)\hat{a}^+\hat{a} + \hbar\lambda\sum_l(\hat{a}\hat{\sigma}_l^+ + \hat{a}^+\hat{\sigma}_l^-) + \sum_l\frac{\hbar(\Omega_l - \omega)}{2}\hat{\sigma}_{l,z} + F(\hat{a} + \hat{a}^+)$$

Lindblad evolution and stationary in RWA ($\hbar = 1$), superoperator size $N^2 \times N^2$

$$\partial_t\hat{\rho} = -\frac{i}{\hbar}[\hat{H}, \hat{\rho}] + \mathcal{L}_d(\rho)$$

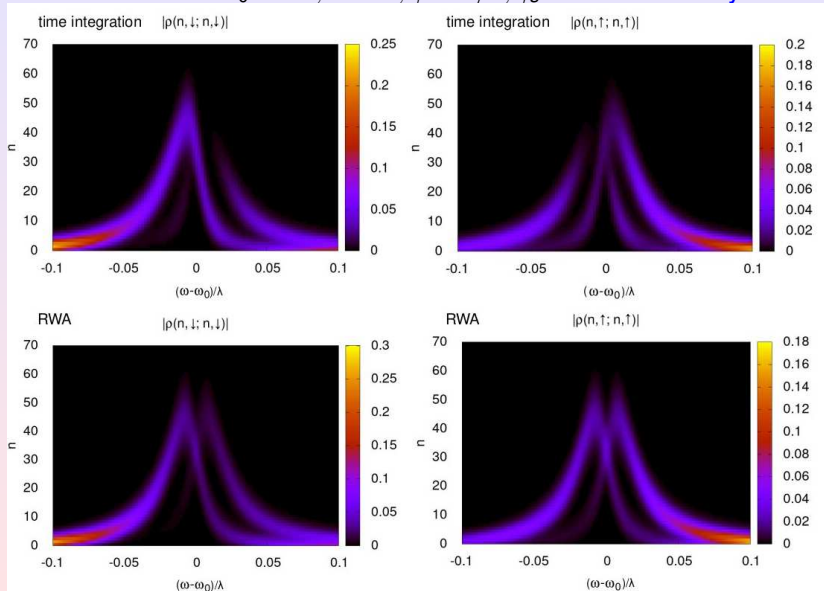
$$\mathcal{L}_d(\hat{\rho}) = \gamma\left(\hat{a}\hat{\rho}\hat{a}^+ - \frac{1}{2}\hat{a}^+\hat{a}\hat{\rho} - \frac{1}{2}\hat{\rho}\hat{a}^+\hat{a}\right) + \gamma_s\sum_l\left(\hat{\sigma}_l^-\hat{\rho}\hat{\sigma}_l^+ - \frac{1}{2}\hat{\sigma}_l^+\hat{\sigma}_l^-\hat{\rho} - \frac{1}{2}\hat{\rho}\hat{\sigma}_l^+\hat{\sigma}_l^-\right)$$

$$\partial_t\hat{\rho}_{\mathcal{R}} = -\frac{i}{\hbar}[\hat{H}_{\mathcal{R}}, \hat{\rho}_{\mathcal{R}}] + \mathcal{L}_d(\rho_{\mathcal{R}})$$

= 0

RWA vs time evolution: resonator + qubit

parameters: $\Delta = \Omega - \omega_0 = 2\lambda$, $F = \lambda$, $\gamma = \lambda/3$, $\gamma_s = 0 \rightarrow$ bistability



QSYNC of qubit with driving phase

parameters: $\Delta_1 = \Omega_1 - \omega_0 = \lambda$, $F = \lambda$, $\gamma = \lambda/3$, $\gamma_s = 0$

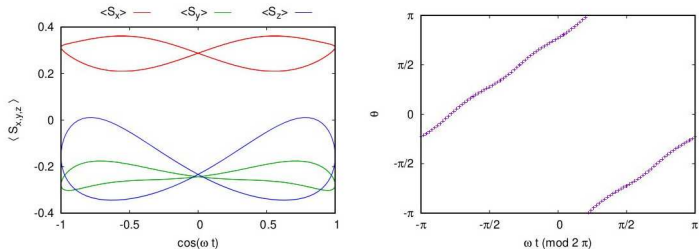


FIG. 15: Synchronization between a driven cavity and a qubit in the system steady-state for $\Delta_1 = \Omega_1 - \omega_0 = \lambda$, $F = \lambda$, $\gamma = \lambda/3$ and RWA parameter $\omega_0/\lambda = 10$. The qubit is non dissipative $\gamma_s = 0$ and data is obtained by integration of Lindblad dynamics. Due to the moderate value of the RWA parameter vibrations around the mean RWA values of the spin projections are clearly visible on the left panel. Right hand panel shows the synchronisation between the angle $\theta = \arg\langle S_x + iS_y \rangle$ of the qubit in plane spin projection and the phase of the cavity driving field.

Semi-analytical methods (RWA)

- * - M1: Rate equation perturbation theory: weak damping γ
- * - M2: semiclassical approximation at strong damping

$$S = \text{Tr} [\mathcal{L}(\hat{\rho})]^+ \mathcal{L}(\hat{\rho}) \quad (31)$$

We first consider the simple model of a driven dissipative cavity in RWA:

$$\hat{H} = \omega_r \hat{a}^+ \hat{a} + F(\hat{a} + \hat{a}^+) \quad (32)$$

$$\mathcal{L}(\hat{\rho}) = [\mathcal{L}(\hat{\rho})]^+ = -i[\hat{H}, \hat{\rho}] + \gamma \left(\hat{a} \hat{\rho} \hat{a}^+ - \frac{1}{2} \hat{a}^+ \hat{a} \hat{\rho} - \frac{1}{2} \hat{\rho} \hat{a}^+ \hat{a} \right) \quad (33)$$

where $\omega_r = \omega_0 - \omega$ is the detuning between the cavity frequency and the driving field F at frequency ω .

We consider a trial density matrix given by a pure coherent state parameterized by complex $\alpha = \alpha_x + i\alpha_y$ (α_x and α_y are the real and imaginary parts of α):

$$\hat{\rho}_\alpha = |\alpha\rangle\langle\alpha| \quad (34)$$

where $\hat{a}|\alpha\rangle = \alpha|\alpha\rangle$.

The functional Eq. (31) can then be evaluated as:

$$S_0(\alpha) = S(|\alpha\rangle\langle\alpha|) = 2 \left[F^2 + 2F\alpha_x\omega_r + (\alpha_x^2 + \alpha_y^2)\omega_r^2 \right] + 2F\alpha_y\gamma + \gamma^2 \frac{\alpha_x^2 + \alpha_y^2}{2} \quad (35)$$

The first bracketed term comes from the Hamiltonian dynamics while the other terms include damping effects.

...

M1 Results at weak damping

driven resonator and 1 qubit

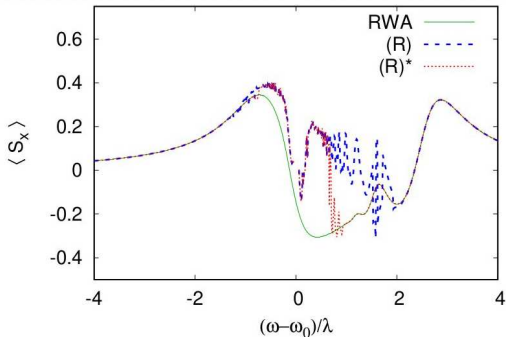


FIG. 3: Comparison of RWA simulation with the summation of rate equation series for $F = \lambda$, $\Omega - \omega_0 = 2\lambda$ and $\gamma = \gamma_s = 0.3\lambda$. The trace (R) corresponds to summation of the series from the direct rate expansion Eq. (19) while (R)* exhibiting a larger radius of convergence corresponds to Eq. (30). The series (R) qualitatively reproduce the position of the multiphoton resonances but with excessive amplitude and fails to converge. The series (R)* reproduce multiphoton resonance accurately but still fail to converge close to the cavity resonance $(\omega - \omega_0)/\lambda \sim 1$ (further studies are needed to know if divergence occurs on energy scale λ or γ around the resonance).

M2 Results at strong damping

driven resonator and 2 qubits

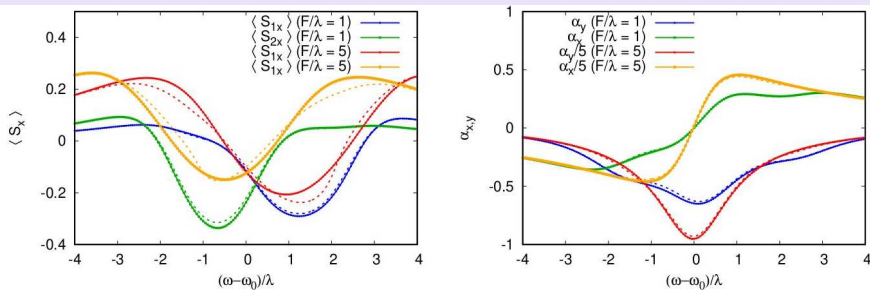


FIG. 5: Spin projections of the two spins as function of the detuning $(\omega - \omega_0)/\lambda$ for excitation strength $F = \lambda$ and $F = 5\lambda$. Dashed lines show the spin projection predicted by the semiclassical functional Eq. (38), dotted lines show the RWA steady state. The qubit-cavity detunings are: $\Delta_1 = \Omega_1 - \omega_0 = 2\lambda$, $\Delta_2 = \Omega_2 - \omega_0 = -\lambda$. The dissipation is fixed to $\gamma = \gamma_s = 2\lambda$, the relatively large value of the dissipation rates ensures good agreement with the semiclassical predictions.

Two entangled dissipative qubits

driven resonator and 2 entangled dissipative qubits

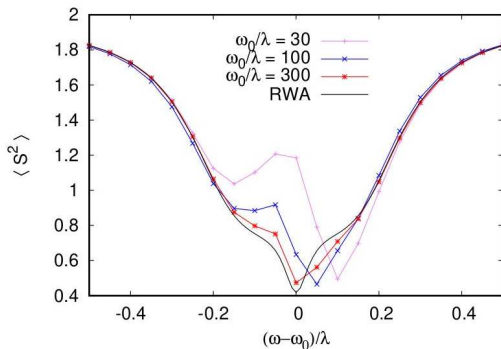


FIG. 8: When dissipative rates are reduced compared to Fig. 7 the reduction of $\langle S^2 \rangle$ for antisymmetric qubit-cavity detunings $\Delta_1 = -\Delta_2 = \lambda$ becomes stronger and the singlet state of the qubit pair becomes the most probable state (75% singlet probability at the minimum of $\langle S^2 \rangle$). Here, the driving strength is set to $F/\lambda = 0.25$, the dissipative rates are $\gamma = 0.3\lambda$ with a weak qubit dissipation $\gamma_s = 10^{-3}\gamma$ (for these parameters, at resonance, $\langle n \rangle \simeq 4F^2/\gamma^2 \simeq 3$). To confirm that the singlet formation is not an artifact of the RWA (black curve), we performed direct integration of the time dependent Lindblad dynamics up to total simulation time $3\gamma_s^{-1}$ for increasing RWA parameter ω_0/λ (color curves with symbols). The singlet formation is robust to non RWA effects with the minimum $\langle S^2 \rangle$ remaining unchanged as ω_0/λ is varied by an order of magnitude. Only weak Non RWA effects are visible as a small shift of the minimum from $\omega = \omega_0$ and an asymmetric $\langle S^2 \rangle$ dependence, since non RWA effects break the symmetry between two anti-symmetrically detuned qubits.

Two entangled dissipative qubits

driven resonator and 2 entangled dissipative qubits

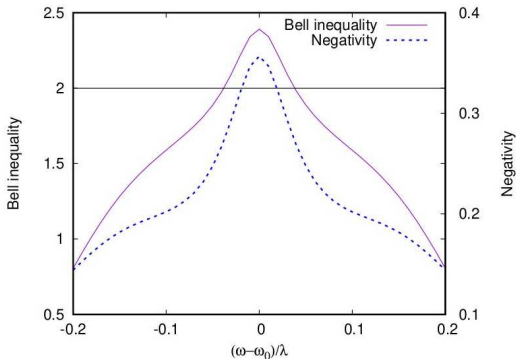


FIG. 9: Bell inequality violation and negativity of the steady-state RWA qubit pair with the reduced density matrix (trace over the cavity) for the parameters of Fig. 8. Since the qubit pair is in a mixture of singlet and triplet states, the polarizability choice for the Bell inequality has to be adjusted to observe a Bell inequality violation (see Appendix and also Fig. 14) there Maximal negativity for two qubits is $1/2$ ^[50] and thus this steady-state shows a high degree of stationary entanglement despite dissipative decoherence of both qubits and cavity.

Two entangled dissipative qubits

driven resonator and 2 entangled dissipative qubits
comparison with semi-analytical methods M1,M2

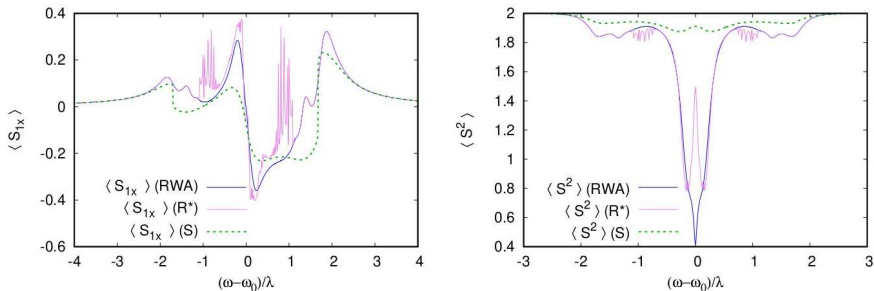


FIG. 10: We test here if our two semi-analytic approaches can reproduce singlet formation for antisymmetric detuning presented in Figs. 8,9. The left panel shows the RWA spin projection $\langle S_{1x} \rangle$ for the first qubit compared with the rate equation series and the variational approximation, the right panel shows the mean total spin $\langle S^2 \rangle$. While both approaches reproduce some qualitative features, they both fail to describe the singlet formation at $\omega - \omega_0 = 0$.

QSYNC of several dissipative qubits

good description by semiclassical method M2

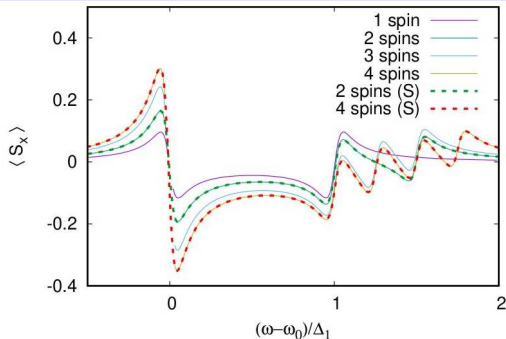


FIG. 16: RWA calculation of total spin projection $\langle S_x \rangle$ as function of the excitation frequency-cavity detuning for an increasing number of qubits coupled to the cavity (full lines). The cavity-qubit interaction is weak $\lambda = \gamma/2$. The qubit-cavity detunings are set to $\Delta_1 = 10\gamma^{-1}$, $\Delta_2 = 15\gamma^{-1}$, $\Delta_3 = 12.5\gamma^{-1}$, $\Delta_4 = 17.5\gamma^{-1}$ (only the first qubits are kept when the number of qubits is smaller than four). Qubit dissipation rate is $\gamma_s = \gamma$ and excitation is $F/\gamma = 2.2$. In this weak interaction regime the semiclassical calculation (shown as dashed lines for 2 and 4 spins) coincides almost exactly with RWA.

Discussion

We show that the synchronization of several qubits with driving phase can be obtained due to their coupling to resonator.

We establish the existence of two different regimes of qubit synchronization: in the first one the semiclassical approach describes well the dynamics of qubits and thus their quantum features and entanglement are suppressed by dissipation and the synchronization is essentially classical, in the second one the entangled steady-state of a pair of qubits remains synchronized in presence of dissipation and decoherence corresponding to the regime non-existing in the classical synchronization.

Diffusion and Localization in a Dissipative Quantum System

Albert Schmid

*Institut für Theorie der Kondensierten Materie, Universität Karlsruhe, D-7500 Karlsruhe,
Federal Republic of Germany*

(Received 1 August 1983)

The motion of a quantum mechanical particle is studied in the presence of a periodic potential and frictional forces. Depending on the parameters, the behavior changes from diffusion to localization.

+ S.A.Bulgadaev *Pis'ma ZhETF* 39, 264 (1984)

EXPERIMENTS:

CEA Saclay experiment: we find that a Josephson junction connected to a resistor does not become insulating beyond a given value of the resistance due to a dissipative quantum phase transition, as is commonly believed.

PRX 10, 021003 (2020)

Manucharyan group experiment: we finally demonstrate this transition by observing the resistor's internal dynamics.

arXiv:2304.05806 April (2023)

OPPOSITE STATEMENTS ???